Simultaneously enhanced stability and biological activities of chlorogenic acid by covalent grafting with soluble oat β-glucan

Yan Luo [a,1], Yun-Cheng Li [a,b,1], Fan-Bing Meng [a,*], Zheng-Wu Wang [b], Da-Yu Liu [a], Wei-Jun Chen [c], Long-Hua Zou [a]

[a] College of Food and Biological Engineering, Chengdu University, Chengdu 610106, PR China
[b] Shanghai Jiao Tong University Sichuan Research Institute, Chengdu 610218, PR China
[c] Key Laboratory of Coarse Cereal Processing, Ministry of Agriculture and Rural Affairs, Chengdu 610106, PR China

ARTICLE INFO

ABSTRACT

Chlorogenic acid (CA) has a wide range of biological activities but the chemical structure is extremely unstable. In this study, CA was grafted onto a soluble oat β-glucan (OβGH) to improve the stability. Although the crystallinity and thermal stability of CA-OβGH conjugates reduced, the storage stability of CA significantly improved. The DPPH and ABTS scavenging ability of CA-OβGH IV (graft ratio 285.3 mg CA/g) were higher than 90 %, which is closed to activities of equivalent concentration of Vc (93.42 %) and CA (90.81 %). The antibacterial abilities of CA-OβGH conjugates are improved compared to the equivalent content of CA and potassium sorbate. Particularly, the inhibition rate of CA-OβGH for gram-positive bacteria (*Staphylococcus aureus* and *Listeria monocytogenes*) are significantly higher than that of gram-negative bacteria (*Escherichia coli*). The results demonstrated that covalent grafted CA with soluble polysaccharide is an effective strategy to enhance its stability and biological activities.

1. Introduction

Foodborne illness is the most prominent public safety problem in the world today. It is estimated that 600 million (7.69 %) of the world population suffer from foodborne illnesses each year, and 420,000 (7.5 %) of all deaths annually are due to foodborne illness (Lee & Yoon, 2021). Microbes are the main cause of food-borne diseases and are ubiquitous (Hammond et al., 2015). The major cause of bacterial foodborne illnesses are pathogens involving enterohemorrhagic *Escherichia coli*, *Listeria monocytogenes*, *Staphylococcus aureus*, etc. Therefore, developing safe and effective bacteriostatic technologies is an important research issue in the food industry. Recently, the antimicrobial nanomaterials technologies based on metal and metal oxides (silver, copper, gold, zinc, etc) have attracted much attention (Abu Elella et al., 2021; Khan, Goda, Rehman, & Sohail, 2021). However, considering the use of metal nanoparticles may cause environmental hazards, the concept of "without chemically synthesized preservatives added" has attracted much attention from consumers (Raybaudi-Massilia, Mosqueda-Melgar, Soliva-Fortuny, & Martin-Belloso, 2009). In addition, facing the growing

reality of bacterial resistance and the side effects of synthetic chemical preservatives (Meng et al., 2022c), it is vital to develop novel and safe natural preservatives to be used in food (Meng et al., 2022a).

Chlorogenic acid (CA, 5-O-caffeoylquinic acid) is a phenolic compound of the hydroxycinnamic acid family with a chemical structure that includes a caffeic acid moiety and a quinic acid moiety (Santana-Gálvez, Cisneros-Zevallos, & Jacobo-Velázquez, 2017). CA is widely distributed in fruits, vegetables, and herbs. The main pharmacological effects of CA are antibacterial, anti-inflammatory, antiviral, and antioxidant (Miao & Xiang, 2020). A previous study demonstrated that CA has antibacterial activity against a wide range of foodborne pathogenic microorganisms, such as bacteria, yeast, molds, and so on (Santana-Gálvez et al., 2017), but it did not inhibit probiotics at high concentrations of 10 mg/mL (Puupponen-Pimiä et al., 2001) Therefore, CA can be used as a natural antibacterial compound in the food industry to preserve food. However, the CA application is limited in the food industry by its low bioavailability and stability. In addition, CA is unstable in light and heat and is easily enzymatically oxidized to quinines by polyphenol oxidase during food processing. Therefore, it is necessary to

---

develop steady-state technologies for CA. In recent years, the synthesis of phenolic acid polysaccharide conjugates by grafting phenolic acids with good antioxidant and antibacterial activities onto the main chain of polysaccharides has attracted the attention of scientists (Zhang, Yu, Diao, & Jing, 2021). More importantly, the stability of CA was significantly improved after grafting modification, so its application range was increased. For example, Fu et al. (2017) demonstrated that the antioxidant activity of CA-gelatin was higher than that of free CA, and the antibacterial activity of CA-gelatin was not affected by conjugation.

Oat is favored by consumers as a multigrain with high nutritional value, which is mainly due to the presence of oat beta-glucan. Oat β-glucan is a polymer consist of β-d-glucopyranosyl units linked by β-(1 → 4) and β-(1 → 3) glycosidic bonds (Li et al., 2022). The β-glucans may contribute to nutritional and functional enhancement and are commonly used to stabilize phenolic acids by as an encapsulation (Li et al., 2022). However, high molecular weight polysaccharides are limited in biological applications due to their low solubility and poor processability. Previous studies have shown that acid degradation can reduce the molecular weight and viscosity of oat β-glucan and enhance solubility and biological activity, especially antioxidant and antibacterial activity (Qin et al., 2021). However, there were few researches had been reported on the modification of polyphenols with low molecular soluble oat β-glucan. Therefore, in this study, the molecular weight of oat β-glucan was reduced by acid degradation, and then the EDC/NHS coupling strategy was adopted to synthesize CA-OβGH conjugates with different grafting ratios. The chemical structure and physical properties of the products were characterized. Stability and antibacterial activity against *S. aureus*, *L. monocytogenes*, and *E. coli* were also investigated. The purpose of this study is to develop an effective strategy to improve water solubility and enhance the stability and biological activities of chlorogenic acid.

2. Materials and methods

2.1. Materials and chemicals

S. aureus, L. monocytogenes and *E. coli* were purchased from Beijing Biobw Biotechnology Co., ltd. (Beijing, China). Crude oat β-glucan (purity 80 %) was obtained from Yikang Biotechnology Co., ltd. (Zhangjiakou, China). Chlorogenic acid (purity 98 %), a1-ethyl-3-(3-dimethylaminopropyl) carbodiimide hydrochloride (EDC, purity 99 %), *N*-hydroxysuccinimide (NHS, purity 99 %), morpholineethanesulfonic acid (anhydrous) (MES, purity 99 %), potassium ferricyanide ($K_3[Fe(CN)_6]$, purity 99.5 %), dialysis membrane (molecular weight cutoff of 3000 Da) were obtained from Shanghai Yuanye Bio-Technology Co., ltd. (Shanghai, China). 2,2-Diphenyl-1-picrylhydrazyl (DPPH) was obtained from Sigma-Aldrich Chemical Co. (St. Louis, MO, USA). 2,2′-Azinobis (3-ethylbenzothiazoline-6-sulfonic acid ammonium salt, ABTS) was obtained from Shanghai Hualan Chemical Technology Co., ltd. (Shanghai, China). All other chemicals were of analytical reagent grade unless otherwise stated.

2.2. Preparation of acid-degraded oat β-glucan

Acid-degraded oat β-glucan (OβGH) was prepared according to previously method (Qin et al., 2021). Briefly, 25 g oat β-glucan was added to 500 mL ultra-pure water (preheated to 90 °C) and stirred for 2 h. Added 100 mL HCl (3 mol/L) to the reaction system with a final concentration of 0.5 mol/L. Stirring at 90 °C for reaction 5 h and then cooled to room temperature, and the pH of the solution adjusted to 7.0 with NaOH (1.0 mol/L). The resulting neutral solution was dialyzed (3000 Da) against ultra-pure water for 3 days and finally freeze-dried to obtain OβGH.

2.3. Synthesis of chlorogenic acid-grafted OβGH conjugates

Chlorogenic acid-grafted OβGH (CA-OβGH) conjugates were synthesized by the EDC/NHS coupling method. OβGH was dissolved in 30 mL of ultra-pure water and stirred for 12 h at room temperature to ensure complete dissolution. a certain amount of CA and EDC were dissolved in 30 mL MES buffer (pH 5.5) and reacted for 10 min to obtain intermediate 1. NHS was added to intermediate 1, and after 1 h in an ice bath reaction, intermediate 2 was obtained. Intermediate 2 was gradually added to the preprepared OβGH solution and stirred at ambient temperature in the dark for 24 h. The final product obtained was dialyzed against distilled water with a 3000 Da molecular weight cutoff membrane for 3 d, and the water changed several times to ensure that there was no free CA in the system. The dialysate was centrifuged at $10,000 \times g$ for 30 min after dialysis, and the supernatant was lyophilized and stored at 4 °C for further analysis. Four different graft rates of CA-OβGH I, CA-OβGH II, CA-OβGH III, and CA-OβGH IV were obtained by setting the fixed molar ratio of CA/EDC/NHS to 1:2:2, and the mass ratios of OβGH and CA were set to 3:1, 3:2, 3:4, and 3:6, respectively.

2.4. Determination of the grafting ratio of CA-OβGH

The polyphenol content of CA-OβGH conjugates was evaluated by the Folin-Ciocalteu method. Five milligrams of CA-OβGH conjugates was dissolved in 10 mL ultra-pure water. Then, the sample solution (1.0 mL) was mixed with a 10-fold dilution of Folin–Ciocalteu reagent (1.0 mL) and left to react at 30 °C for 5 min in the dark. After incubation, 2.0 mL Na_2CO_3 solution (20 %, w/v) was added, and the mixture further incubated in the dark at room temperature for 1 h. The absorbance of the reaction mixture was determined at 760 nm by a full wavelength microplate reader (Thermo Fisher Scientific, MA, USA). Taking CA as the standard of the calibration curve, the grafting ratio of CA-OβGH conjugates was expressed as mg of CA equivalent per g dried sample (mg/g) and calculated as in Eqn. (1):

$$Grafting\ ratio = \frac{C_1 * 1000}{C_0} \tag{1}$$

where C_1 represents the calculated total phenolic content of the CA-OβGH solution based on the standard curve of CA (mg/mL), and C_0 represents the concentration of the CA-OβGH solution (0.5 mg/mL).

2.5. Characterization of CA-OβGH

2.5.1. Fourier transform infrared spectroscopy (FTIR) analysis

CA, OβG, OβGH, and CA-OβGH conjugates were detected using a Spectrum two FT-IR spectrometer (PerkinElmer, Waltham, MA, USA) in a wavenumber range of 400–4000 cm^{-1} (Meng, Li, Liu, Zhong, & Guo, 2018). The resolution was 4 cm^{-1}, and the scanning time was 32. The background was removed with a blank chip. The samples were ground and mixed with KBr (1:120, w/w) and pressed into tablets for analysis.

2.5.2. UV–vis spectrum

The UV–vis at 200–600 nm of CA, OβG, OβGH, and CA-OβGH conjugates were determined by UV–vis spectrophotometer spectrum (UV-2700i, Shimadzu, China).

2.5.3. X-ray diffraction (XRD) analysis

XRD patterns of samples were identified by using a Bruker D8 Advance diffractometer (Karlsruhe, Germany) with Cu Kα radiation at 40 kV and 40 mA. The scanning scope was set from 4° to 40° at a step size of 0.02°, and the and scanning speed was set at 2 s and 2°/min, respectively.

2.5.4. Thermogravimetric analysis

The thermal properties of CA, OβG, OβGH, and CA-OβGH conjugates

were recorded on an STA 449F3 TGA/DSC instrument (NETZSCH, Free State of Bavaria, Germany). Dried samples (10 mg) were heated from 30 °C to 600 °C at a heating rate of 10 °C/min under a nitrogen flow of 50 mL/min in an alumina pan (Yu et al., 2021).

2.5.5. ^1H NMR analysis

The ^1H NMR spectra were used to analyze the structural properties. The CA, OβG, OβGH, and CA-OβGH conjugates were dissolved in 0.5 mL D_2O and 0.1 mL DMSO. ^1H NMR spectra were acquired at ambient temperature on a Bruker UltraShield (500 MHz) spectrometer (D8 ADVANCE, Bluker, Germany).

2.6. Storage stability evaluation

The storage stability of the samples was investigated according to the method of Li et al. (2018) with some modifications: CA-OβGH conjugates were dissolved in distilled water to make the effective CA concentration reach 30 μg/mL. All samples were kept at room temperature, and a UV–visible light spectrophotometer was used to scan the samples in the range of 200–400 nm once a week. The maximum absorbance was recorded and used to evaluate the stability.

2.7. In vitro antioxidant activities analysis

2.7.1. DPPH radical scavenging activity

The DPPH radical scavenging activities of the CA, OβG, OβGH, and CA-OβGH conjugates were investigated according to the method of (Rao, Meng, Li, Chen, Liu & Zhang, 2022). All samples were dissolved in ultra-pure water at concentrations of 0.2, 0.4, 0.6, 0.8 and 1.0 mg/mL. Pipetting 100 μL test sample mixed with 100 μL 0.1 mmol/L DPPH methanol solution in a 96-well plate, the reaction system was kept in the dark at room temperature and stand for 30 min. The absorbance of the reaction solution was determined at 517 nm using a Synergy H1 microplate reader (BioTek, VT, USA).

2.7.2. ABTS radical scavenging activity

The ABTS radical scavenging activity was investigated according to the description of Meng et al. (2022b). Equal volumes of ABTS solution (7 mmol/L) and $K_2S_2O_8$ (2.45 mmol/L) were blended and kept in the dark for 14 h. The reaction solution was diluted with phosphate buffer (0.2 mol/L, pH 7.4) to an absorbance of 0.70 ± 0.02 at 734 nm. After that, 30 μL of test samples were blended with 170 μL ABTS solution in a 96-well plate and incubated in the dark for 10 min at 25 °C. The absorbance was determined at 734 nm.

2.7.3. Hydroxyl radical scavenging activity

The hydroxyl radical scavenging activity was analyzed according to Zhu et al., (2022): 0.1 mL of ferrous sulfate solution (9 mmol/L), 0.1 mL of salicylic acid–ethanol solution (9 mmol/L) and 1.0 mL of sample solution (0.2–1.0 mg/mL) were added to the test tube. Then, 0.1 mL of hydrogen peroxide (8.8 mmol/L) was added to start the reaction after incubation in a water bath at 37 °C for 30 min. The mixture was centrifuged at 8000×g for 6 min to remove the precipitated polysaccharide. The absorbance of the supernatant was detected at 510 nm.

2.7.4. Ferric reducing antioxidant power

Iron reduction antioxidant capacity was carried out according to the method described by Zhang, Tan, Zhao, Mi, & Guo (2022). Samples (0.5 mL) of different concentrations (1.0, 2.0, 3.0, 4.0 and 5.0 mg/mL) were mixed with 0.5 mL of potassium ferricyanide solution 1 % (w/v), and then incubated at 50 °C for 20 min. After cooling, 0.5 mL of 10 % (w/v) trichloroacetic acid was added, mixed and centrifuged at 8000×g for 10 min. The supernatant (0.5 mL) was collected and 0.5 mL of distilled water and 0.1 mL of ferric chloride solution 0.1 % (w/v) were added and mixed well. The absorbance of the mixture was detected at 700 nm after incubating at room temperature for 10 min.

2.8. Antimicrobial activity analysis

2.8.1. Activation and cultivation of strains

Two kinds of gram-positive *S. aureus*, *L. monocytogenes* and one kind of gram-negative *E. coli* were used in this study. Pipetted 200 μL of the activated strain broth and inoculated into LB broth (1 % tryptone, 0.5 % yeast extract and 1 % NaCl, pH 7.2–7.4), incubated at 37 °C and 160 r/min for 12–16 h to the logarithmic phase, which is first-generation solutions. The first-generation solutions were incubated on LB agar plates (LB broth with 2 % agar) for 16 h, and a single colony was transferred to a new LB broth and cultured at 37 °C to the logarithmic phase to obtain the second-generation solution.

2.8.2. Antibacterial activity evaluation by plate count

The antimicrobial effects of CA, OβG, OβGH, and CA-OβGH conjugates were measured by the plate counting method following previously described procedures (Majidiyan et al., 2022) with slight modifications. The final bacterial suspensions were obtained by diluting the second-generation solutions to 10^5 CFU/mL with physiological saline (0.9 %, w/v). Under sterile conditions, the bacterial suspension was inoculated (2.5 μL) into 5.00 mL of LB broth containing 2 mg/mL OβG, OβGH, CA-OβGH I, CA-OβGH II, CA-OβGH III, and CA-OβGH IV, equivalent to 0.1, 0.2, 0.4, and 0.6 mg/mL CA, respectively. Meanwhile, potassium sorbate preservative was used as a control. The samples were incubated at 37 °C and 160 r/min for 6 h, and then 50 μL of the cultures were pipetted evenly coating LB plates. After 16 h incubation, photographs were taken to record the results.

2.8.2. Antibacterial activity evaluation by growth curve

The growth curve was assessed by an optical density (OD_{600}) method. Fresh second-generation solution was diluted to $OD_{600} = 0.05$ (approximately 10^7 CFU/mL) and 100 μL of the dilutions and 100 μL of 4 mg/mL samples were pipetted and added to a 96-well plate. The blank was prepared by adding 100 μL dilutions and 100 μL sterilized LB broth. All samples were incubated at 37 °C and 160 r/min. The OD_{600} of the mixture was recorded at different time. The bacterial growth behavior was represented by the relative OD value, which was obtained by subtracting the OD value at time T_0 from the OD value at any later time. The inhibiting rate at 12 h (IR_{12}) cultivation was calculated as in Eqn. (2):

$$IR_{12} = \left(1 - \frac{B_{12} - B_0}{A_{12} - A_0}\right) \times 100\% \tag{2}$$

where A_0 is OD_{600} of the blank at time T_0, A_{12} is OD_{600} of the blank at time T_{12}, B_0 is OD_{600} of the culture treated with CA-OβGH at time T_0, B_{12} is OD_{600} of the culture treated with CA-OβGH at time T_{12}.

2.9. Statistical analysis

Data were analyzed by using IBM SPSS Statistics 20.0 (IBM Corporation, Somers, NY, USA). Data are expressed as the mean ± standard deviation (SD). Statistical differences were performed by oneway analysis of variance (ANOVA). Duncan's test was performed to compare the means, and differences were considered significant at $p < 0.05$.

3. Results and discussion

3.1. Preparation of CA-OβGH conjugates

The high molecular weight of OβG limits its biological application due to its low solubility and poor processability, so the molecular weight of oat β-glucan was reduced by acid degradation from 1.3×10^5 to 4581. In this study, the molar ratio of CA:EDC:NHS was fixed at 1:2:2, and CA-OβGH conjugates with different grafting ratios were prepared by changing the mass ratio of OβGH:CA to 3:1, 3:2, 3:4 and 3:6. The final products CA-OβGH I, CA-OβGH II, CA-OβGH III and CA-OβGH IV with

grafting ratios of 50.9, 106.1, 199.5, and 285.3 mg CA/g, respectively, were obtained, and all of them show good solubility.

3.2. Structural characterization of CA-OβGH conjugates

3.2.1. FT-IR characterization

As shown in Fig. 1A. CA exhibited typical phenolic characteristics, including a benzene ring single –OH stretching vibration at 3353 cm^{-1}; a mixed ester and carboxyl C═O stretching vibration at 1687 cm^{-1}; benzene ring stretching vibrations at 1638 cm^{-1}, 1602 cm^{-1}, 1518 cm^{-1} and 1443 cm^{-1}; carboxylic C—O—C stretching vibrations at 1287 cm^{-1} and 1188 cm^{-1}; and a carboxylic O—H bending vibration at 603 cm^{-1} (Fu et al., 2017). The FT-IR spectrum of OβG presented three characteristic bands at 3407 cm^{-1}, 2885 cm^{-1}, and 1645 cm^{-1}, which correspond to the stretching absorption bands of poly-OH, C—H and C═O, respectively. The peak at 1072 cm^{-1} was assigned to C—O—C stretching in the OβG structure (Hussain, Rather, & Suradkar, 2018). The absorption peak at 897 cm^{-1} is the angular vibration of the β-pyran ring, which belongs to the characteristic absorption peak of β-glucan (Qian, Chen, Zhang, & Zhang, 2009). The above results indicated that the structures of the main chain of OβG and OβGH were the same, which is consistent with the report of Qin et al. (2021) that acid degradation did not affect the monomeric structure of β-glucan. A new peak at 1732 cm^{-1} formed in CA-OβGH conjugates, and the peak intensity increased with increasing grafting ratio, which indicated that ester bonds were established between the hydroxyl groups of OβGH and the carboxyl groups of CA. New peaks were formed at 1633 cm^{-1}, 1608 cm^{-1}, and 1518 cm^{-1}, and the stretching vibration increased with increasing grafting ratio, while the stretching vibration weakened at 1443 cm^{-1}, which may be related to the main chain vibration of the aromatic nucleus and CA substitution (Wang, Cao, Sun, & Wang, 2011). Besides, peaks with different intensities were formed at 816 cm^{-1}, which is close to the position of 818 cm^{-1} in the main chain of CA, which may be attributed to the function of CA. These alterations provide evidence for the successful formation of CA-OβGH.

3.2.2. UV–vis spectrum characterization

To validate the junctions of functional molecules (CA) on OβGH, the CA-OβGH conjugates were characterized by UV–vis spectroscopy. As shown in Fig. 1B, the absorbance of OβG and OβGH at 200–600 nm had no obvious absorption peaks. CA had two characteristic UV absorption peaks at 260 nm and 331 nm, which are ascribed to the π-system of the phenolic hydroxyl group on the benzene ring (Zhao, Wang, Yang, & Tao, 2010). Compared to OβGH and CA, the CA-OβGH conjugates had no absorption peak at 260 nm, but they had characteristic absorption peaks at 309 nm, 316 nm, and 328 nm, and their spectra show a blueshift. This

result is similar to the shift of the absorption peak at 325.0 nm to a shorter wavelength (316.5 nm) of chitosan-CA covalent complexes (Wei & Gao, 2016). In addition, with the increase in the grafting ratio of CA-OβGH conjugates, the absorption intensity gradually increased, which could preliminarily determine the covalent binding reaction between OβGH and CA.

3.2.3. XRD analysis

As shown in Fig. 2A. The CA monomer showed different sharp and intense diffraction peaks within the 2θ region of 4.8°-30.2°, which indicates its crystalline morphology (Shao, Zhang, Fang, & Sun, 2014). The original OβG presented two characteristic peaks at 2θ values of 11.5° and 20.1°, which indicates that OβG possesses a semicrystalline structure. However, the major diffraction peak of OβGH at approximately 11.8° was enhanced, indicating that the crystal structure of OβGH changed to a certain extent after acid degradation treatment. This result is similar to a previous report in which the irradiated oat β-D-glucan samples showed no significant change in the diffraction pattern except for a decrease in the intensity of X-ray diffraction (Hussain et al., 2018) In comparison with OβGH, new peaks with low intensity appeared at approximately 22.1° in the diffractogram of CA-OβGH conjugates, which is due to the characteristic diffraction peak on CA. This result indicates that the introduction of CA slightly changed the crystalline properties of OβGH. The decrease in the crystallinity of CA-OβGH conjugates may be due to the reduction or destruction of the inter- and intramolecular hydrogen bonds of OβGH during the grafting process. A decrease in crystallinity was also observed in studies of other polyphenol polysaccharide conjugates (Wei & Gao, 2016; Zhang et al., 2021).

3.2.4. Thermal properties of CA-OβGH conjugates

Thermogravimetric analysis could provide a crucial tool for understanding the thermal properties, thermal degradation and weight loss of material with variations in temperature (Shivangi, Dorairaj, Negi, & Shetty, 2021). As shown in Fig. 2B, the thermal degradation of CA is mainly divided into three stages: the first weight loss (2.1 %) observed in the range of 32–148 °C is attributed to evaporation of water; the second step in the range of 149–280 °C weight loss rate of 7.2 %, and the third step occurred in the high temperature region of 281–500 °C with a weight loss rate of 50.8 %. The thermal degradation of OβG is divided into two stages: the weight loss rate of the first stage (32–178 °C) is 4.8 %, which is mainly caused by the evaporation of water. The mass loss rate in the range of 179–500 °C was 72.4 %, which was attributed to the combustion and degradation of the main chain of OβG (Wu et al., 2013). The thermal degradation of OβGH is divided into three stages, the first stage (32–175 °C), the second stage (176–280 °C) and the third stage (281–500 °C). The first DTG shows that the maximum decomposition
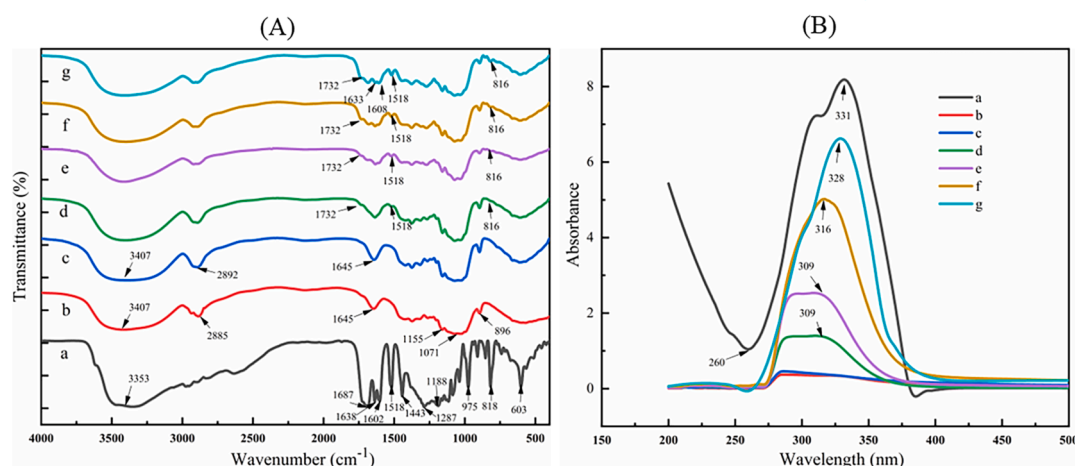

Fig. 1. FT-IR spectra (A) and UV–vis spectra (B) of CA (a), OβG (b), OβGH (c), CA-OβGH I (d), CA-OβGH II (e), CA-OβGH III (f) and CA-OβGH IV (g).
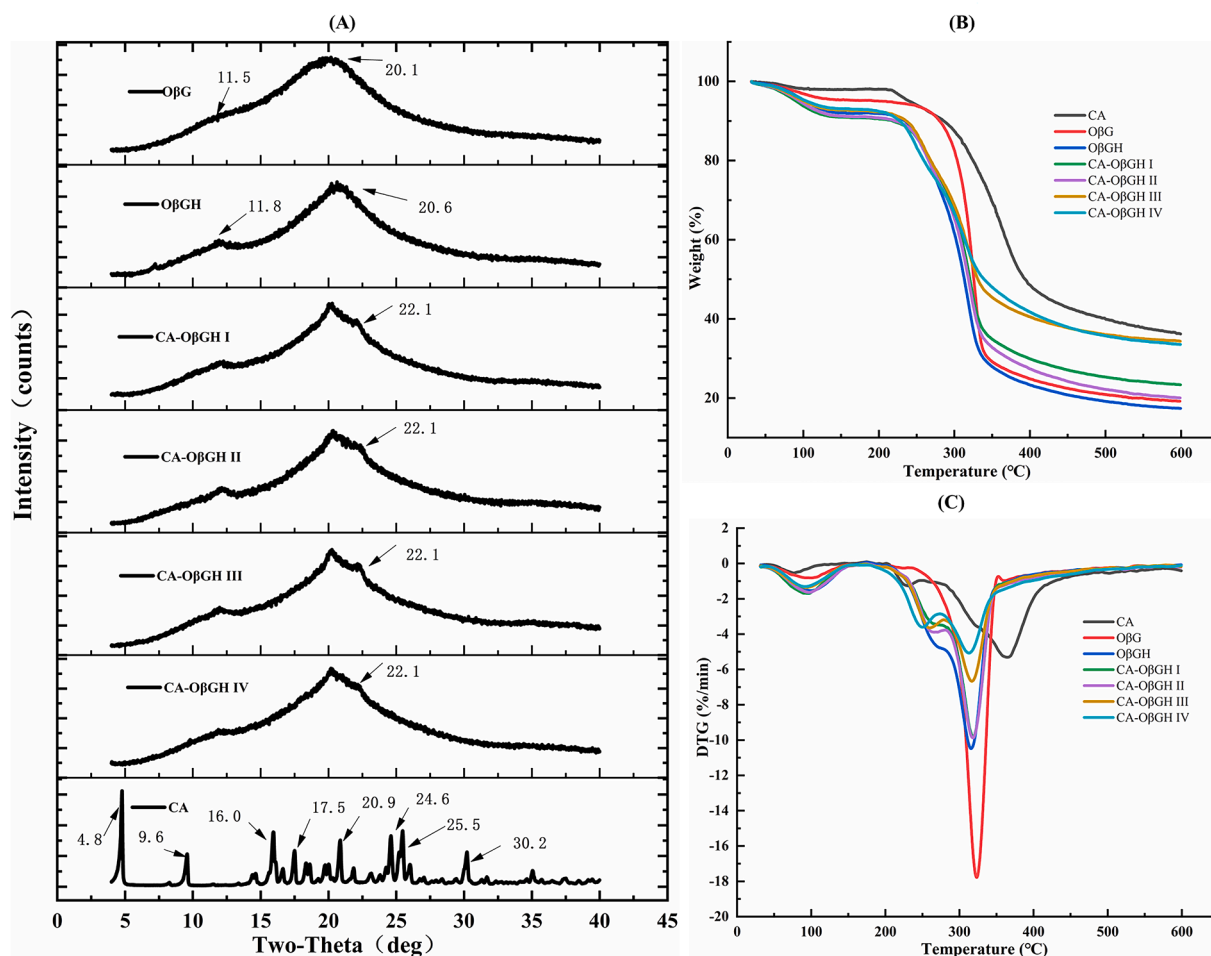
Fig. 2. X-ray diffraction profile (A), TGA thermogram (B) derivative thermogravimetric curves (C) of CA, OβG, OβGH, CA-OβGH I, CA-OβGH II, CA-OβGH III and CA-OβGH IV.

rates of OβG and OβGH appear at 325 °C and 316 °C, respectively ([Fig. 2]C), which indicate that the process of acid degradation reduces the thermal stability ([Liu, Pu, Zhang, Xiao, Kan & Jin, 2018]). The thermal degradation of CA-OβGH conjugates is mainly divided into three stages: The first step is the evaporation of free water (32–175 °C), the second degradation stage is 176–280 °C, and the third stage is 281–500 °C. The DTG results showed that with the increase in grafting ratio, the peak temperature of the sample in the second stage is closer to CA (232 °C), which may be due to the degradation of the grafted CA and the decrease of the decomposition temperature. These results suggest that the intercalation of CA into OβGH may hinder OβGH chain stacking, resulting in slightly lower thermal stability of CA-OβGH conjugates than OβGH, and decreased with the increase in grafting ratio.

3.2.5. ^1H NMR analysis

In order to ascertain the structure of CA-OβGH conjugates, the characterizations of CA, OβG, OβGH and CA-OβGH conjugates were also evaluated by ^1H NMR spectrum. In terms of OβG and OβGH, the characteristic peaks were seen at δ 3.2–3.9 ppm and were assigned to the hydrogen protons on C-2, C-3 to C-6 ([Fig. 3]). The ^1H NMR spectrum of CA at δ 5.15–7.46 ppm revealed five different types of proton signals, specifically, H-a, H-b, H-c (aromatic protons) as well as H-d and H-e (the adjacent CH = CH-protons) ([Chao, Wang, Zhao, Zhang, & Zhang, 2012]), and the peak at 1.98 ppm, 2.12 ppm assigned to the protons on C-g and C-h, respectively ([Suárez-Quiroz, Alonso Campos, Valerio Alfaro, González-Ríos, Villeneuve & Figueroa-Espinoza, 2014]). In addition to all characteristic proton signals of OβGH, the new characteristic spectrum

of CA-OβGH conjugates appeared in the range of 5.14–7.58 ppm, 4.15 ppm, 1.92–2.09 ppm, showing several characteristic absorption peaks related to CA, the signal of the above peak was enhanced with the increase of the grafting ratio of CA-OβGH, which indicated that the co-valent attachment of CA to OβGH was successful.

3.3. Evaluation of the storage stability of CA-OβGH conjugates

The storage stability of CA and the CA-OβGH conjugates were evaluated by detecting the most absorbances during storage in room temperature. As shown in [Fig. 4]A, the absorption values of both CA and CA-OβGH conjugates gradually decreased with storage time. The absorbance of CA-OβGH conjugates was significantly higher than that of CA from 4 weeks onward ($P < 0.05$). The degradation of CA-OβGH conjugates was relatively delayed under visible light and atmospheric temperature compared to that of free CA, which indicated that the insertion of CA into the OβGH backbone can improve the stability of CA. This may be that by combining bioactive molecules within the hydrophobic cavity of OβGH, some reactive functional groups of the guest molecules are protected from potential reactants. The same result was observed in the cyclodextrin/CA inclusion complex studied by [Zhao et al. (2010)]. These results indicated that the polysaccharide-phenolic acid covalent complexes are of great significance for protecting biologically active compounds in delivery systems.
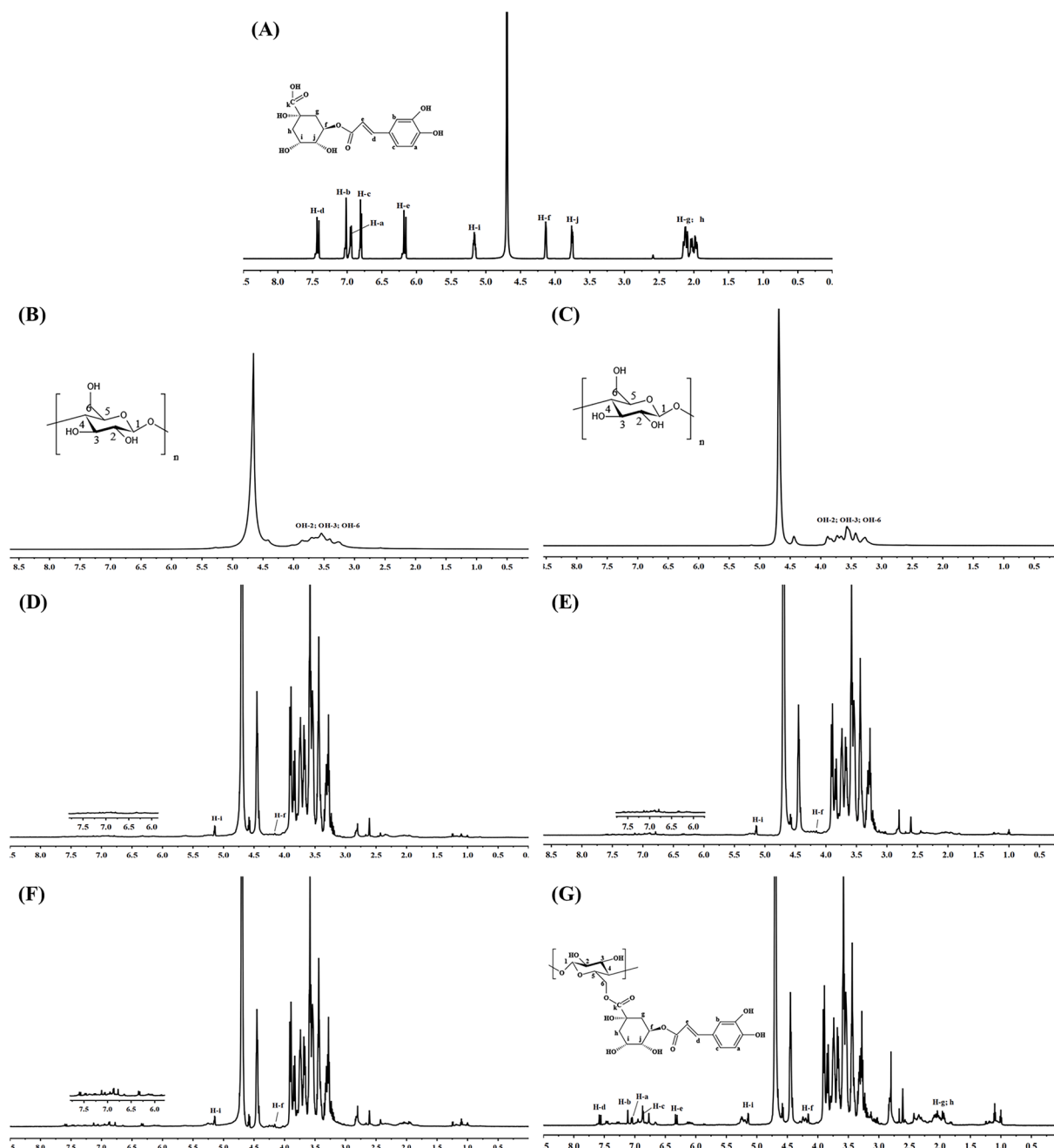
Fig. 3. ^{1}H spectra of CA (A), oat β-glucan (B), OβGH (C), CA-OβGH I (D), CA-OβGH II (E), CA-OβGH III (F), and CA-OβGH IV(G).

3.4. In vitro antioxidant activities of CA-OβGH conjugates

3.4.1. DPPH radical scavenging activity

As shown in Fig. 4(B). The DPPH scavenging ability of OβGH was significantly higher than that of pristine OβG, which may be due to the reduction of hydroxyl exposure and intermolecular hydrogen bonds during acid degradation (Fu, Chen, Dong, Zhang, & Zhang, 2010). Low molecular weight OβG can transfer hydrogen from molecules under physiological conditions, so it has been proven to be a good free radical scavenger (Bai et al., 2019). The DPPH scavenging ability of CA-OβGH conjugates was significantly higher than that of OβGH, and scavenging ability increased with increasing grafting ratios, indicating that the insertion of CA into the OβGH chain plays a crucial role in the DPPH scavenging ability. CA-OβGH conjugates strongly quenched DPPH radicals in a dose-dependent manner. When the CA-OβGH conjugates increased to 0.4 mg/mL, the DPPH scavenging activity of CA-OβGH III

and CA-OβGH IV has arrived to 90.79 %, respectively, which is closed to scavenging activities of equivalent concentration of Vc (93.42 %) and CA (90.81 %). The enhanced free radical scavenging activity of CA-OβGH might be attributed to the hydrogen atom donating and electron transferring ability of CA moieties. Firstly, CA-OβGH can react with DPPH radical by donating hydrogen atom (H•) to form stable DPPH-H and CA-OβGH radical. Then, CA-OβGH radical can further withdrawn hydrogen atom (H•) to eventually form stable CA-OβGH quinone.

3.4.2. ABTS radical scavenging activity

The principle of the ABTS radical scavenging method is that when the electrons in the antioxidant compound are transferred to the ABTS radical, the solution gradually fades to light green or is colorless (Kungel et al., 2018). As shown in Fig. 4(C), the ability of OβGH to scavenge ABTS free radicals is significantly greater than that of OβG, which is consistent with the results of DPPH radical scavenging ability. The ABTS
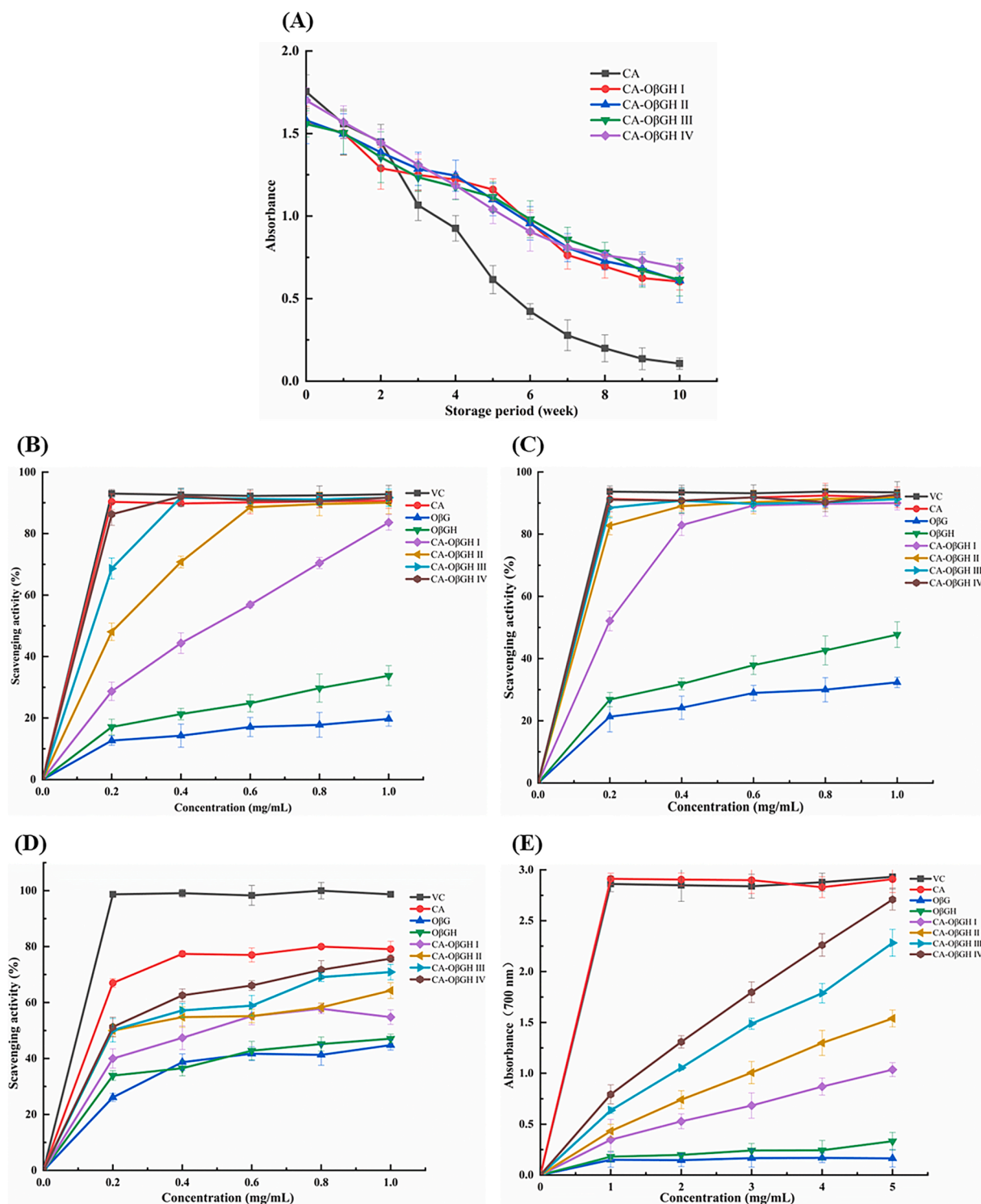
Fig. 4. Storage stability (A) and Antioxidant capacity of (B-E) of CA, OβG, OβGH, CA-OβGH I, CA-OβGH II, CA-OβGH III and CA-OβGH IV. (A), DPPH radical scavenging activity; (B), ABTS radical scavenging activity; (C), hydroxyl radical scavenging activity; (D), Ferric reducing antioxidant power.

scavenging ability of CA-OβGH conjugates was significantly higher than that of OβGH, and scavenging ability increased with increasing grafting ratios. When the concentration of CA-OβG IV reached 0.4 mg/mL, the ABTS radical scavenging ability were 92.08 %, which is similar to the scavenging ability of Vc (92.61 %), but slightly higher than that of CA (89.79). The above results indicate that CA not only retains high anti-oxidant activity but also synergistically exerts antioxidant activity after covalent reaction with OβGH. On the one hand, it is possible that the

reduction of the hydroxy group and intermolecular hydrogen bonds that causes the increased OβGH scavenging activity during degradation (Fu et al., 2010), and on the other hand, the covalent binding of OβGH and CA improves the stability of CA to exert a better antioxidant effect.

3.4.3. Hydroxyl radical scavenging activity

Hydroxyl radical (•OH)is the most active of reactive oxygen species and has extremely strong oxidation ability. The ability of OβGH to

remove •OH before and after graft modification was investigated by the production of •OH with high reactivity under the catalysis of Fe²⁺ by H₂O₂. As shown in Fig. 4(E), the ability of OβGH to scavenge hydroxyl radicals is slightly greater than that of OβG, which may be because acid degradation treatment destroyed the molecular structure of OβG, thereby improving its ability to prevent the chain reaction of •OH (Tang, Huang, Zhao, Zhou, Huang & Li, 2017). The •OH scavenging ability of CA-OβGH conjugates was significantly higher than that of OβGH. When the sample concentration was greater than 0.4 mg/mL, the •OH radical scavenging of CA-OβGH conjugates was significantly higher than that of OβGH. At the same time, the removal effect of all samples is significantly enhanced with the increasing concentration. This indicates that the introduction of CA enhanced the scavenging rate of hydroxyl radicals by CA-OβGH conjugates.

3.4.4. Ferrous reducing power

Reducing ability is an important indicator for judging the potential antioxidant activity of polysaccharides and their derivatives. The antioxidants can reduce K₃[Fe(CN)₆] and then use Fe²⁺ to generate Prussian blue (Fe₄(Fe(CN)₆)), which has a maximum absorption peak at 700 nm (Qi, Zhang, Zhao, Hu, Zhang & Li, 2006). As shown in Fig. 4(F), the reducing power of OβG and OβGH is much lower than that of Vc, but the reducing power of OβGH is slightly higher than that of OβG. The reducing power of the samples did not promote significantly with increasing concentration, which may be attributed to the lower content of electron-donating compounds in the chemical composition of polysaccharides (Romdhane, Haddar, Ghazala, Jeddou, Helbert & Ellouz-Chaabouni, 2017). The reducing power of CA-OβGH conjugates is significantly higher than that of OβGH, and reducing power improved with increase of grafting ratio. At a concentration of 5 mg/mL, the reducing powers of OβGH, CA-OβGH I, CA-OβGH II, CA-OβGH III and CA-OβGH IV were 0.333, 1.036, 1.540, 2.282, and 2.708, respectively.

Totally, it was concluded that the antioxidant activity of CA-OβGH conjugates can be enhanced by incorporating CA into the OβG backbone, especially CA-OβGH IV has strong antioxidant activity. Hence, CA-OβGH conjugates have great potential as antioxidants in food.

3.5. Antimicrobial activity

Foodborne illnesses are a serious food safety concern, and pathogenic microorganisms are the most common cause of food spoilage and are ubiquitous, because they are too small to be observed with the naked eye. In addition to mold, food contaminated with bacteria and yeast may go unnoticed by producers, retailers and consumers (Hammond et al., 2015). Therefore, inhibiting the growth of pathogenic microorganisms is of great significance for food preservation and safety. To determine whether the graft modification could affect the antibacterial activities of CA, the antimicrobial activities were investigated based on the equivalent content of CA in CA-OβGH conjugates. As shown in Fig. 5, the three indicator bacteria were not obviously inhibited by OβG, and OβGH compared to Blank. Potassium sorbate, CA and CA-OβGH conjugates inhibited the growth of *S. aureus*, *L. monocytogenes*, and *E. coli* to varying degrees, and the inhibition of CA-OβGH conjugates was greater than that of the equivalent content of CA and potassium sorbate. In addition, the inhibitory activity of CA-OβGH conjugates increased with the increasing graft ratio, indicating that the antibacterial activity of OβGH was effectively improved after the introduction of CA. Among them, CA-OβGH IV showed the strongest antibacterial activity among the three food pathogens. In addition, the antibacterial effect of CA-OβGH III and CA-OβGH IV was significantly greater than the equivalent content of CA. This result indicates that the antibacterial activity of CA in the CA-OβGH conjugates is not only undiminished but also exerts a synergistic antibacterial effect with OβGH. The increase in antibacterial activity may be related to the acid degradation of oat β-glucan, that leads to the exposure
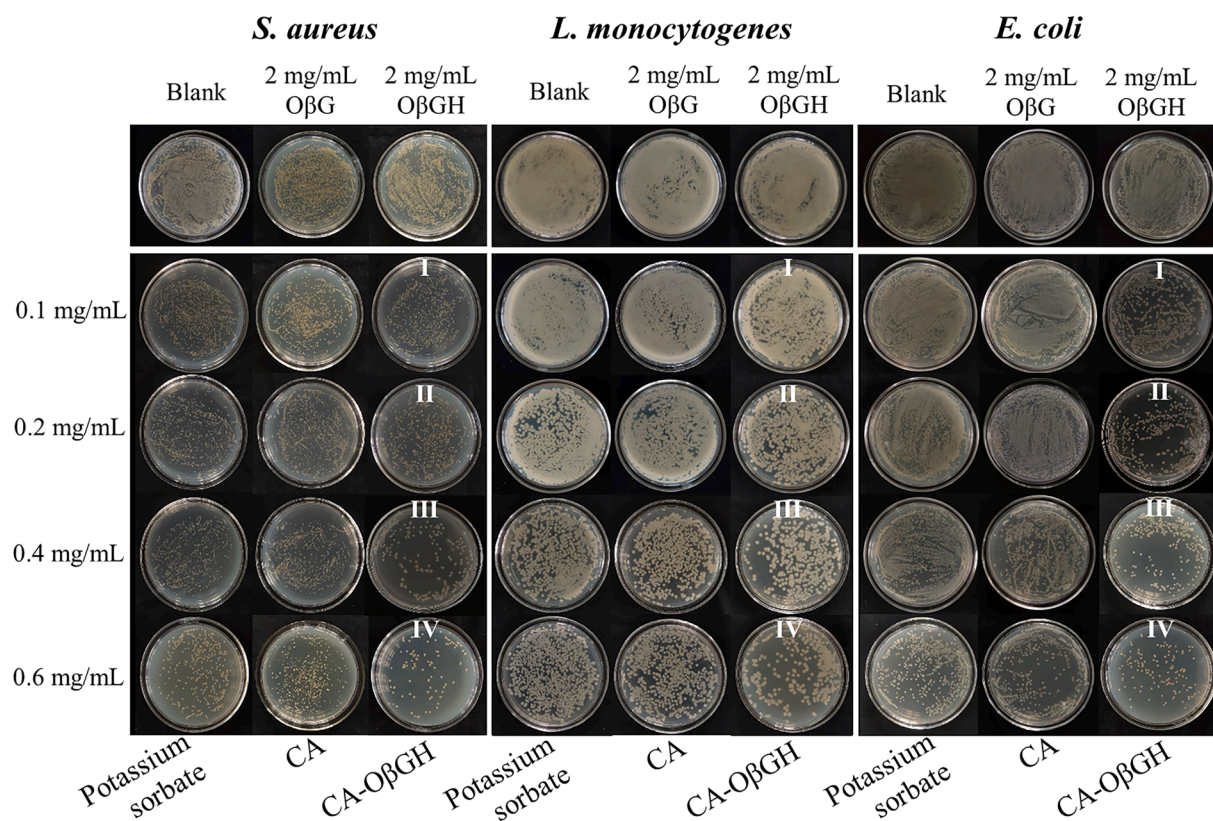

Fig. 5. Growth observations of *S. aureus*, *L. monocytogenes* and *E. coli* in LB plates. The addition amount of CA-OβGH had been converted to CA equivalent according to grafting ratio.

of their hydroxyl groups, and reducing the intermolecular hydrogen bonding. In addition, CA also plays an important role in antibacterial activity.

The time-dependent antibacterial effect of CA and CA-OβGH conjugates were investigated by tracking the absorbance (OD_{600}) changes of bacterial solutions in the absence/presence of 2 mg/mL CA-OβGH conjugates during 4 to 12 h incubation. As shown in Fig. 6A–C, the growth curve of the bacteria treated with OβG was similar to that of the positive control group (without sample), while the relative OD values of the bacterial suspensions treated with OβGH were slightly lower than those of OβG within 12 h, which indicates that natural OβG hardly exhibits antibacterial activity. The chemical modification improved its antibacterial activity. After CA-OβGH conjugate treatment, the relative OD of all tested samples were significantly lower than those of the blank group and OβGH group, which indicated that the antibacterial activity of the CA-OβGH conjugate against all three bacterial strains was improved by grafting CA onto OβGH, and antimicrobial activity increased with the increase in grafting ratio. The inhibition rate further proved this result. As shown in Fig. 6D, the IR_{12} of all CA-OβGH conjugates were significantly higher than that of OβG and OβGH. Meanwhile, the IR_{12} of CA-OβGH I, CA-OβGH II and CA-OβGH III for *S. aureus* significantly higher than that of *L. monocytogenes*, respectively, but CA-OβGH IV showed the same inhibition rate for these two strains. Most importantly, the IR_{12} of CA-OβGH conjugates for both two Gram-positive bacteria (*S. aureus* and *L. monocytogenes*) are significantly higher than that of Gram-negative bacteria (*E. coli*). Similar results have reported that cyclodextrin/CA is most effect against *S. aureus*, second is *B. subtilis* and worst is *E. coli* (Zhao et al., 2010). This may be attributed to the different cell wall composition of bacteria. The cell wall of Gram-positive bacteria (*S. aureus*) consists of a peptidoglycan layer with a large number of pores, so CA and CA-OβGH conjugates molecules can easily bind to the outer bacterial membrane, disrupt and permeabilize the cell membrane, which can lead to leakage of cytoplasmic macromolecules and even cell death (Lou, Wang, Zhu, Ma, & Wang, 2011). However, Gram-negative bacteria (*E. coli*) have a complex bilayer cell structure with a cell wall composed of a thin peptidoglycan layer and an outer layer composed of lipoproteins, lipopolysaccharides, and phospholipids. Therefore, the outer membrane is a potential barrier against CA and CA-OβGH conjugated molecules.

4. Conclusion

In the present study, acid degradation was used to obtain soluble oat β-glucan (OβGH). Through grafting CA onto OβGH, CA-OβGH conjugates with different grafting ratios from 50.9 to 285.3 mg CA/g were successfully prepared. UV–vis, FT-IR, ^{1}H NMR and XRD analysis indicated that CA was successfully grafted onto the OβGH backbone. Although the crystallinity and thermal stability of CA-OβGH were lower
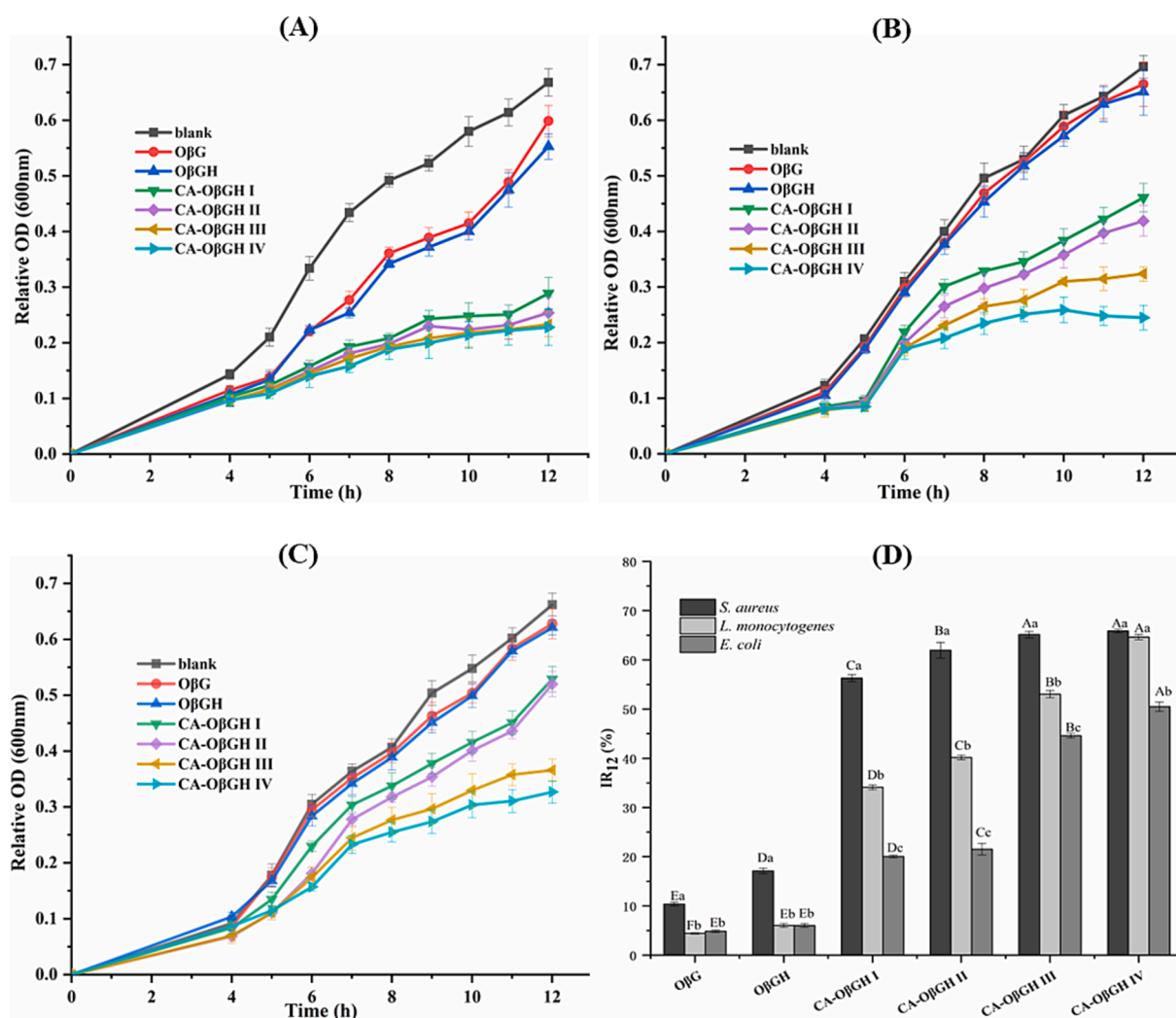

Fig. 6. Growth curve (A-C) and inhibiting rate at 12 h cultivation (IR_{12}) in LB broth medium with 2 mg/mL OβG, OβGH, CA-OβGH I, CA-OβGH II, CA-OβGH III and CA-OβGH IV. (A), *S. aureus*; (B), *L. monocytogenes*; (C), *E. coli*. Different capital letters in (D) represent different significance ($p < 0.05$) of different treatments on the same strain, different lowercase letters in (D) represent different significance ($p < 0.05$) of different strains on the same treatment.

than that of OβGH, the storage stability of CA-OβGH was significantly improved. CA-OβGH showed the same DPPH and ABTS scavenging ability as the equivalent amount of free CA. In addition, compared with OβGH and the equivalent amount of free CA, CA-OβGH had stronger antibacterial activities against *S. aureus*, *L. monocytogenes*, and *E. coli*. The antibacterial activity increased with increasing grafting ratios, and the inhibition rate of CA-OβGH conjugates for Gram-positive bacteria (*S. aureus* and *L. monocytogenes*) are significantly higher than that of Gram-negative bacteria (*E. coli*). The above results indicated that CA-OβGH may have the potential as an antioxidant and antibacterial agent in food applications.

CRediT authorship contribution statement

Yan Luo: Data curation, Writing – original draft. **Yun-Cheng Li:** Conceptualization, Methodology, Writing – original draft. **Fan-Bing Meng:** Writing – review & editing, Visualization, Supervision. **Zheng-Wu Wang:** Resources, Funding acquisition. **Da-Yu Liu:** Writing – review & editing, Funding acquisition. **Wei-Jun Chen:** Data curation, Project administration. **Long-Hua Zou:** Formal analysis.

Declaration of Competing Interest

The authors declare that they have no known competing financial interests or personal relationships that could have appeared to influence the work reported in this paper.

Data availability

No data was used for the research described in the article.

Acknowledgment

References

Abu Elella, M. H., Goda, E. S., Gamal, H., El-Bahy, S. M., Nour, M. A., & Yoon, K. R. (2021). Green antimicrobial adsorbent containing grafted xanthan gum/SiO2 nanocomposites for malachite green dye. *International Journal of Biological Macromolecules, 191*, 385–395. https://doi.org/10.1016/j.ijbiomac.2021.09.040

Bai, J., Ren, Y., Li, Y., Fan, M., Qian, H., Wang, L., … Rao, Z. (2019). Physiological functionalities and mechanisms of β-glucans. *Trends in Food Science & Technology, 88*, 57–66. https://doi.org/10.1016/j.tifs.2019.03.023

Chao, J., Wang, H., Zhao, W., Zhang, M., & Zhang, L. (2012). Investigation of the inclusion behavior of chlorogenic acid with hydroxypropyl-β-cyclodextrin. *International Journal of Biological Macromolecules, 50*(1), 277–282. https://doi.org/10.1016/j.ijbiomac.2011.11.008

Fu, L. L., Chen, H. X., Dong, P., Zhang, X., & Zhang, M. (2010). Effects of ultrasonic treatment on the physicochemical properties and DPPH radical scavenging activity of polysaccharides from mushroom *Inonotus obliquus*. *Journal of Food Science, 75*(4), C322-C327. 10.1111/j.1750-3841.2010.01590.x.

Fu, S., Wu, C., Wu, T., Yu, H., Yang, S., & Hu, Y. (2017). Preparation and characterisation of chlorogenic acid-gelatin: A type of biologically active film for coating preservation. *Food Chemistry, 221*, 657–663. https://doi.org/10.1016/j.foodchem.2016.11.123

Hammond, S. T., Brown, J. H., Burger, J. R., Flanagan, T. R., Fristoe, T. S., Mercado-Silva, N., … Okie, J. G. (2015). Food spoilage, storage, and transport: Implications for a sustainable future. *Bioscience, 65*(8), 758–768. https://doi.org/10.1093/biosci/biv081

Hussain, P. R., Rather, S. A., & Suradkar, P. P. (2018). Structural characterization and evaluation of antioxidant, anticancer and hypoglycemic activity of radiation degraded oat (*Avena sativa*) β- glucan. *Radiation Physics and Chemistry, 144*, 218–230. https://doi.org/10.1016/j.radphyschem.2017.08.018

Khan, Z. A., Goda, E. S., Rehman, A., & Sohail, M. (2021). Selective antimicrobial and antibiofilm activity of metal–organic framework NH2-MIL-125 against Staphylococcus aureus. *Materials Science and Engineering: B, 269*, Article 115146. https://doi.org/10.1016/j.mseb.2021.115146

Kungel, P. T. A. N., Correa, V. G., Corrêa, R. C. G., Peralta, R. A., Soković, M., Calhelha, R. C., … Peralta, R. M. (2018). Antioxidant and antimicrobial activities of a purified polysaccharide from yerba mate (*Ilex paraguariensis*). *International Journal of Biological Macromolecules, 114*, 1161–1167. https://doi.org/10.1016/j.ijbiomac.2018.04.020

Lee, H., & Yoon, Y. (2021). Etiological agents implicated in foodborne illness world wide. *Food Science of Animal Resources, 41*(1), 1–7. https://doi.org/10.5851/kosfa.2020.e75

Li, Y.-C., Luo, Y., Meng, F.-B., Li, J., Chen, W.-J., Liu, D.-Y., … Zhou, L. (2022). Preparation and characterization of feruloylated oat β-glucan with antioxidant activity and colon-targeted delivery. *Carbohydrate Polymers, 279*, Article 119002. https://doi.org/10.1016/j.carbpol.2021.119002

Li, Y. C., Zhong, G., Meng, F. B., Yu, H., Liu, D. Y., & Peng, L. X. (2018). Konjac glucomannan octenyl succinate (KGOS) as an emulsifier for lipophilic bioactive nutrient encapsulation. *Journal of the Science of Food and Agriculture, 98*(15), 5742–5749. https://doi.org/10.1002/jsfa.9122

Liu, J., Pu, H., Zhang, X., Xiao, L., Kan, J., & Jin, C. (2018). Effects of ascorbate and hydroxyl radical degradations on the structural, physicochemical, antioxidant and film forming properties of chitosan. *International Journal of Biological Macromolecules, 114*, 1086–1093. https://doi.org/10.1016/j.ijbiomac.2018.04.021

Lou, Z. X., Wang, H. X., Zhu, S., Ma, C. Y., & Wang, Z. P. (2011). Antibacterial activity and mechanism of action of chlorogenic acid. *Journal of Food Science, 76*(6), M398–M403. https://doi.org/10.1111/j.1750-3841.2011.02213.x

Majidiyan, N., Hadidi, M., Azadikhah, D., & Moreno, A. (2022). Protein complex nanoparticles reinforced with industrial hemp essential oil: Characterization and application for shelf-life extension of Rainbow trout fillets, *Food Chemistry: X, 13*, 2022, 100202. 10.1016/j.fochx.2021.100202.

Meng, F.-B., Gou, Z.-Z., Li, Y.-C., Zou, L.-H., Chen, W.-J., & Liu, D.-Y. (2022a). The efficiency of lemon essential oil-based nanoemulsions on the inhibition of *Phomopsis* sp. and reduction of postharvest decay of kiwifruit. *Foods, 11*(10), 1510. 10.3390/foods11101510.

Meng, F.-B., Zhou, L., Li, J.-J., Li, Y.-C., Wang, M., Zou, L.-H., … Chen, W.-J. (2022b). The combined effect of protein hydrolysis and *Lactobacillus plantarum* fermentation on antioxidant activity and metabolomic profiles of quinoa beverage. *Food Research International, 157*, Article 111416. https://doi.org/10.1016/j.foodres.2022.111416

Meng, F. B., Lei, Y. T., Zhang, Q., Li, Y. C., Chen, W. J., & Liu, D. Y. (2022c). Encapsulation of *Zanthoxylum bungeanum* essential oil to enhance flavor stability and inhibit lipid oxidation of Chinese-style sausage. *Journal of the Science of Food and Agriculture., 102*, 4035–4045. https://doi.org/10.1002/jsfa.11752

Meng, F. B., Li, Y. C., Liu, D. Y., Zhong, G., & Guo, X. Q. (2018). The characteristics of konjac glucomannan octenyl succinate (KGOS) prepared with different substitution rates. *Carbohydrate Polymers, 181*, 1078–1085. https://doi.org/10.1016/j.carbpol.2017.11.040

Miao, M., & Xiang, L. (2020). Chapter Three - Pharmacological action and potential targets of chlorogenic acid. In G. Du (Ed.), *Advances in Pharmacology* (pp. 71–88). Academic Press.

Puupponen-Pimiä, R., Nohynek, L., Meier, C., Kähkönen, M., Heinonen, M., Hopia, A., & Oksman-Caldentey, K.-M. (2001). Antimicrobial properties of phenolic compounds from berries. *Journal of Applied Microbiology, 90*(4), 494–507. https://doi.org/10.1046/j.1365-2672.2001.01271.x

Qi, H., Zhang, Q., Zhao, T., Hu, R., Zhang, K., & Li, Z. (2006). *In vitro* antioxidant activity of acetylated and benzoylated derivatives of polysaccharide extracted from *Ulva pertusa* (Chlorophyta). *Bioorganic & Medicinal Chemistry Letters, 16*(9), 2441–2445. https://doi.org/10.1016/j.bmcl.2006.01.076

Qian, J. Y., Chen, W., Zhang, W. M., & Zhang, H. (2009). Adulteration identification of some fungal polysaccharides with SEM, XRD, IR and optical rotation: A primary approach. *Carbohydrate Polymers, 78*(3), 620–625. https://doi.org/10.1016/j.carbpol.2009.05.025

Qin, Y., Xie, J., Xue, B., Li, X., Gan, J., Zhu, T., & Sun, T. (2021). Effect of acid and oxidative degradation on the structural, rheological, and physiological properties of oat β-glucan. *Food Hydrocolloids, 112*, Article 106284. https://doi.org/10.1016/j.foodhyd.2020.106284

Rao, J.-W., Meng, F.-B., Li, Y.-C., Chen, W.-J., Liu, D.-Y., & Zhang, J.-M. (2022). Effect of cooking methods on the edible, nutritive qualities and volatile flavor compounds of rabbit meat. *Journal of the Science of Food and Agriculture, 102*(10), 4218–4228. https://doi.org/10.1002/jsfa.11773

Raybaudi-Massilia, R. M., Mosqueda-Melgar, J., Soliva-Fortuny, R., & Martin-Belloso, O. (2009). Control of pathogenic and spoilage microorganisms in fresh-cut fruits and fruit juices by traditional and alternative natural antimicrobials. *Comprehensive Reviews in Food Science and Food Safety, 8*(3), 157–180. https://doi.org/10.1111/j.1541-4337.2009.00076.x

Romdhane, M. B., Haddar, A., Ghazala, I., Jeddou, K. B., Helbert, C. B., & Ellouz-Chaabouni, S. (2017). Optimization of polysaccharides extraction from watermelon rinds: Structure, functional and biological activities. *Food Chemistry, 216*, 355–364. https://doi.org/10.1016/j.foodchem.2016.08.056

Santana-Gálvez, J., Cisneros-Zevallos, L., & Jacobo-Velázquez, D. A. (2017). Chlorogenic acid: Recent advances on its dual role as a food additive and a nutraceutical against metabolic syndrome. *Molecules, 22*(3), 358. https://doi.org/10.3390/molecules22030358

Shao, P., Zhang, J., Fang, Z., & Sun, P. (2014). Complexing of chlorogenic acid with β-cyclodextrins: Inclusion effects, antioxidative properties and potential application in grape juice. *Food Hydrocolloids, 41*, 132–139. https://doi.org/10.1016/j.foodhyd.2014.04.003

Shivangi, S., Dorairaj, D., Negi, P. S., & Shetty, N. P. (2021). Development and characterisation of a pectin-based edible film that contains mulberry leaf extract and its bio-active components. *Food Hydrocolloids, 121*, Article 107046. https://doi.org/10.1016/j.foodhyd.2021.107046

Suárez-Quiroz, M. L., Alonso Campos, A., Valerio Alfaro, G., González-Ríos, O., Villeneuve, P., & Figueroa-Espinoza, M. C. (2014). Isolation of green coffee chlorogenic acids using activated carbon. *Journal of Food Composition and Analysis, 33*(1), 55–58. https://doi.org/10.1016/j.jfca.2013.10.005

Tang, Q., Huang, G., Zhao, F., Zhou, L., Huang, S., & Li, H. (2017). The antioxidant activities of six (1→3)-β-d-glucan derivatives prepared from yeast cell wall. *International Journal of Biological Macromolecules, 98*, 216–221. https://doi.org/10.1016/j.ijbiomac.2017.01.132

Wang, J., Cao, Y. P., Sun, B. G., & Wang, C. T. (2011). Characterisation of inclusion complex of trans-ferulic acid and hydroxypropyl-beta-cyclodextrin. *Food Chemistry, 124*(3), 1069–1075. https://doi.org/10.1016/j.foodchem.2010.07.080

Wei, Z., & Gao, Y. (2016). Evaluation of structural and functional properties of chitosan chlorogenic acid complexes. *International Journal of Biological Macromolecules, 86*, 376–382. https://doi.org/10.1016/j.ijbiomac.2016.01.084

Wu, C., Chu, B., Kuang, L., Meng, B., Wang, X., & Tang, S. (2013). Synthesis of β-1,3-glucan esters showing nanosphere formation. *Carbohydrate Polymers, 98*(1), 807–812. https://doi.org/10.1016/j.carbpol.2013.06.056

Yu, J., Chen, G., Zhang, Y., Zheng, X., Jiang, P., Ji, H., … Chen, Y. (2021). Enhanced hydration properties and antioxidant activity of peanut protein by covalently binding with sesbania gum via cold plasma treatment. *Innovative Food Science and Emerging Technologies, 68*, Article 102632. https://doi.org/10.1016/j.ifset.2021.102632

Zhang, C. H., Yu, X. Q., Diao, Y. J., & Jing, Y. J. (2021). Functionalization of carboxymethyl chitosan with chlorogenic acid: Preparation, characterization, and antioxidant capacity. *Iranian Polymer Journal, 30*(1), 81–91. https://doi.org/10.1007/s13726-020-00875-9

Zhang, J., Tan, W., Zhao, P., Mi, Y., & Guo, Z. (2022). Facile synthesis, characterization, antioxidant activity, and antibacterial activity of carboxymethyl inulin salt derivatives. *International Journal of Biological Macromolecules, 199*, 138–149. https://doi.org/10.1016/j.ijbiomac.2021.12.140

Zhao, M., Wang, H., Yang, B., & Tao, H. (2010). Identification of cyclodextrin inclusion complex of chlorogenic acid and its antimicrobial activity. *Food Chemistry, 120*(4), 1138–1142. https://doi.org/10.1016/j.foodchem.2009.11.044

Zhu, Z., Chen, J., Chen, Y., Ma, Y., Yang, Q., Fan, Y., … Liao, W. (2022). Extraction, structural characterization and antioxidant activity of turmeric polysaccharides. *LWT - Food Science and Technology, 154*, Article 112805. https://doi.org/10.1016/j.lwt.2021.112805